Electromagnetic Science
vol. 3, no. 2, 0100583, June 2025
https://doi.org/10.23919/emsci.2024.0058

RESEARCH ARTICLE

Antenna Thousandfold Miniaturization with Ohmic-Biased Transistor Circuit

Shuyu Wang[1†], Yongjian Zhang[1†], Zhenyu Liu[1†], Jinlong Zhang[2], Ziheng Zhou[3], Wenhua Chen[1,2], Zhijun Zhang[1,2], Xi Chen[2], Kunpeng Wei[4], and Yue Li[1,2]

1. *Department of Electronic Engineering*, *Tsinghua University*, *Beijing 1000084*, *China*
2. *Beijing National Research Center for Information Science and Technology*, *Beijing 100084*, *China*
3. *College of Physics and Information Engineering*, *Fuzhou University*, *Fuzhou 350108*, *China*
4. *Xiaomi Communication Company Ltd.*, *Beijing 100085*, *China*

Corresponding author: Yue Li, Email: lyee@tsinghua.edu.cn.
†Shuyu Wang, Yongjian Zhang, and Zhenyu Liu contributed equally to this work.
Received November 6, 2024; Accepted March 26, 2025; Published Online April 14, 2025.

Abstract — Antennas are essential components of any wireless system due to their irreplaceable functions in transmitting and receiving electromagnetic waves. Antenna radiation is based on the free electron resonance, leading to a concrete relation between its physical size and operating frequency. This fundamental principle makes it unrealizable to design well-radiated antennas with extremely small dimensions, e.g., milli-wavelength scales. Here, to overturn this commonsense correlation, an extremely miniaturization methodology of antennas is developed by integrating an arbitrary-sized antenna with an ohmic-biased transistor (OBT) circuit. In this way, we thousandfold miniaturize the antenna to an overall size at milli-wavelength scales, including the OBT circuits. Proven by the experiments in the demonstration systems, the wireless system with this thousandfold miniaturized antenna receives electromagnetic waves well. This methodology would be widely utilized in space-limited wireless systems that cannot provide enough space for antennas, benefiting various exciting areas, such as information technologies, photoelectricity physics, biomedical science, and so on.

Keywords — Miniaturized antennas, Ohmic region, Field effect transistors.
Citation — Shuyu Wang, Yongjian Zhang, Zhenyu Liu, *et al.*, "Antenna thousandfold miniaturization with ohmic-biased transistor circuit," *Electromagnetic Science*, vol. 3, no. 2, article no. 0100583, 2025. doi: 10.23919/emsci.2024.0058.

I. Introduction

Antennas play a crucial role in electromagnetic (EM) wave-based radio systems, serving as the interface between the physical environment and radio-frequency (RF) circuits [1]–[4]. Space-limited wireless systems, such as wearable devices, implant sensors, and drone-carried terminals, require antennas with extremely small dimensions [5]–[8]. However, conventional antennas operate on the free electron resonance, which involves interconnected resonance of free electrons within the antenna and the propagating EM wave [9]–[11]. This resonance is characterized by a specific electric field distribution across the antenna body, resulting in a pronounced correlation between the resonance wavelength and the physical dimensions of the antennas [12]–[14]. As a conceptual demonstration, Figure 1(a) illustrates a conventional antenna with length *L*. When an EM wave is impinging on the antenna, part of energy is reflected and the remainder is received and transmitted to the systems. A maximum transmission, characterized by low reflection and high gain, is achieved with strong resonant behavior, which occurs when the antenna length is comparable to the wavelength of EM wave, as shown in Figures 1(b) and 1(c). This size-frequency correlation is the fundamental physics across all types of antennas [15]–[19], including EM, optic, and acoustic antennas. Consequently, this intrinsic relationship poses a significant challenge in designing well-radiated antennas with extremely small dimensions. To address this bottleneck, two conceptual pathways have been explored for realizing miniaturized antennas: the use of special materials and active circuits. Representing the material method, magnetoelectric (ME) antennas are constructed based on a magnetostrictive/piezoelectric heterostructure [20]–[22],

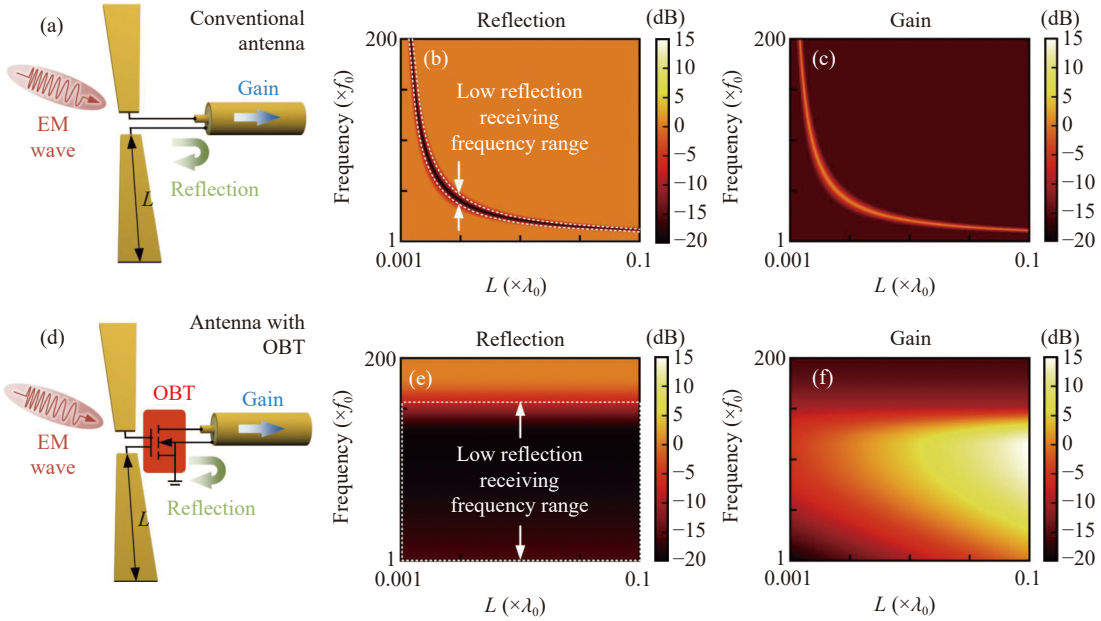

Figure 1 Principles of conventional antenna (a)–(c) and OBT antenna (d)–(f). (a) Schematic of a conventional antenna; (b) Reflection of the conventional antenna in terms of the length L (The effective receiving frequency form an inverse proportion with L); (c) Gain of the conventional antenna in terms of the length L; (d) Schematic of the OBT antenna; (e) Reflection of the OBT antenna in terms of the length L; (f) Gain of the OBT antenna in terms of the length L. λ_0 and f_0 stand for the free-space wavelength and operating frequency, respectively.

which emits EM wave through voltage-controlled deformation, achieving a scale of 2 milli-wavelengths (excluding the coil for magnetic field bias). However, the ME coupling possesses a high quality factor, limiting the operating frequency of the ME antennas to a narrow bandwidth of 0.3% [21]. Additionally, the magnetic bias coils add extra bulk, while causing incompatibility with wireless systems based on printed circuit board (PCB) structures. As an alternative, the active circuit approach has been proposed to construct effective components with negative impedance characteristics (e.g., negative capacitance and inductance), known as non-Foster circuits [23]–[26]. Miniaturized antennas have been realized using non-Foster impedance matching circuits [27]–[29], but demand complex circuit structures with multiple transistors, significantly increasing their physical dimensions and power consumption. Therefore, a pervasive methodology distinct from ME antennas and non-Foster circuits for achieving antennas with extremely miniaturized size, wide operating bandwidth, and high PCB compatibility is still highly desirable.

To develop a wireless system with an extremely miniaturized antenna, we develop the methodology of ohmic-biased transistor (OBT) integration [30], [31], which is to integrate an arbitrary-sized antenna element with the OBT circuit. Reference [30] detailed the engineering realization of the hundred-octave antenna using OBT matching technology. Mathematical derivation and experimental analysis validate that enlarging the antenna element size has a minor effect on its operating frequency but significantly increases the receiving gain. This finding overturns the fundamental physics on size-frequency relation of antennas. With this method, designers can select the size of the antenna part based solely on the gain requirement, without concern for the operating frequency. Further utilizing this exotic feature of OBT antennas, we minimize the antenna element to a limit and reduce it to a microstrip line with the length and width being 1.36 mm and 0.75 mm ($0.00045\lambda_0$ and $0.00025\lambda_0$ at 100 MHz), respectively, resulting in an overall size at milli-wavelength scale, including the OBT circuit. This approach minimizes the antenna's size to the point where it occupies no additional space on the circuit board, and is comparable to the size of a chip or solder pad. Measurements validate that the miniaturized OBT antenna possesses a wide frequency range with well-radiated performances of low reflection and high gain. Moreover, demonstration systems are constructed to validate the performance of the miniaturized OBT antenna in real-life scenarios, including a sound transmission system and a video transmission system. Both wireless systems exhibit excellent radiating performance, indicating the potential of this miniaturized antenna to play a crucial role in cutting-edge fields such as information technologies [32], photoelectricity physics [33], [34], and other disciplines [35], [36].

II. Results

1. Theory of OBT integration

Figure 1(d) shows the conceptual schematic of the antenna with OBT integration. In this configuration, the antenna element is connected to the gate of the OBT, while the port is connected to the drain. The drain impedance of a transistor increases from 0 to ∞ as the drain bias voltage increases. Therefore, a suitable bias configuration can be established in the ohmic region to reach a near 50 Ω drain impedance,

ensuring a matched impedance. Through this configuration, the operating frequency of the antenna with OBT integration is primarily determined by the OBT, thus resulting in a geometry-irrelevant antenna. Unlike conventional RF amplifiers, the OBT functions as an impedance matching component, matching the impedance between a small antenna and the transmission line to cancel the return loss. This results in a broader operating bandwidth. By minimizing return loss due to impedance mismatch, the OBT increases the gain, not by amplifying the signal, but through improved impedance matching. As conceptually illustrated in Figure 1(e), altering the antenna length L has a minor effect on the operating frequency of the OBT antenna. Conversely, increasing the antenna length significantly enhances its receiving gain, as shown in Figure 1(f). This distinctive characteristic is in stark contrast to conventional resonance-based antennas, as represented by Figures 1(a)–1(c).

The impedance and gain features of the OBT antenna can be derived utilizing the equivalent circuit model proposed in [30], [31]. Figure 2(d) presents the model of the antenna with OBT integration. In this model, the antenna is represented as a voltage source V_A with internal impedance $Z_A = R_A + jX_A$, where R_A and X_A stand for the real and imaginary part of the impedance, respectively. The OBT is modeled as a voltage-controlled current source g_m with a gate capacitor C_G and a channel resistor R_D. Parasitic capacitors C_C and C_D are also included to account for the non-ideality of the OBT. Using this model, the impedance of the antenna with OBT integration is derived as follows [37]:

$$Z_{\mathrm{OBT}} = \frac{1}{\frac{1}{R_D} + j\omega C_D + K(Z_A)} \tag{1}$$

where $K(Z_A)$ represents the impact of the antenna element impedance Z_A on the overall impedance of the OBT antenna, and ω stands for the angular frequency. The factor $K(Z_A)$ can be detailly expressed as

$$K(Z_A) = j\omega C_C \times \frac{\frac{1}{Z_A} + j\omega C_G + g_m}{\frac{1}{Z_A} + j\omega(C_G + C_C)} \tag{2}$$

Equation (2) indicates that the impact factor $K(Z_A)$ is

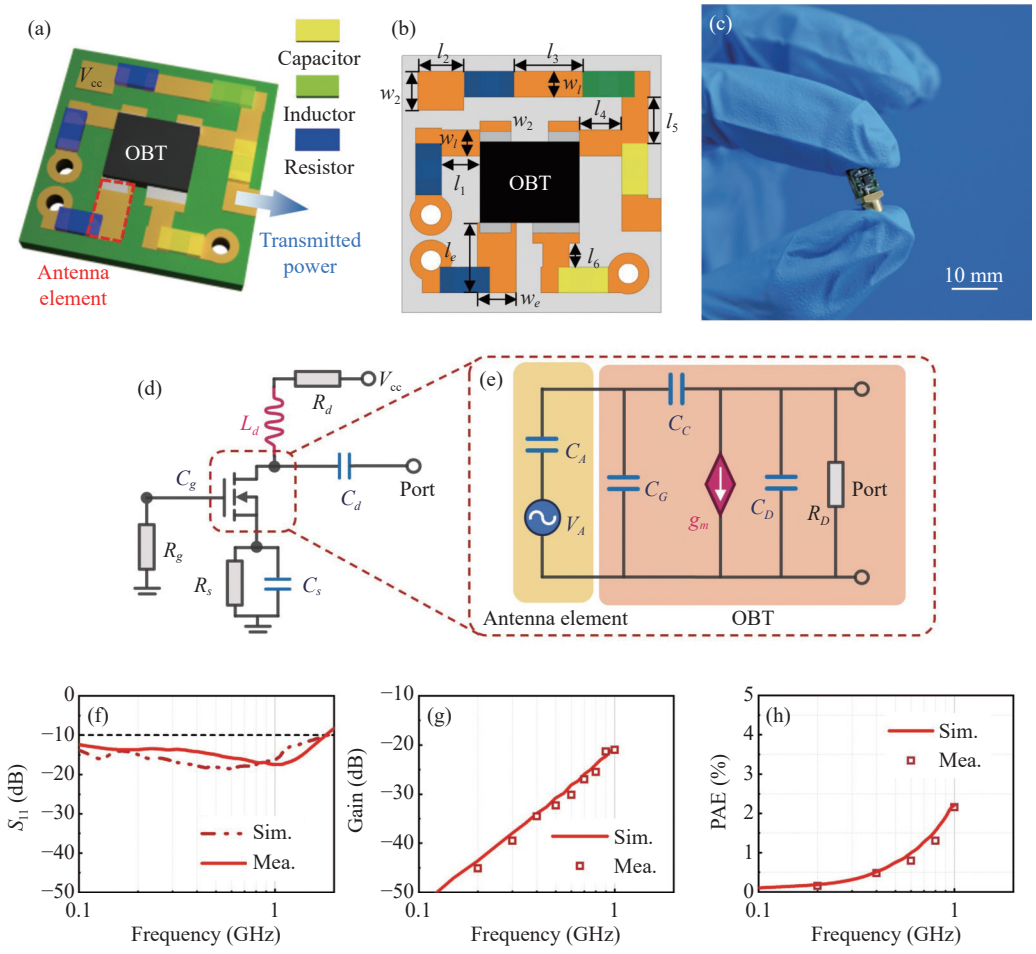

Figure 2 Experimental demonstrations of miniaturized OBT antenna. (a) Schematic of the miniaturized OBT antenna. The antenna element is minimized to a microstrip line, labeled in red frame; (b) Top view of the miniaturized OBT antenna with sizes labeled; (c) Photograph of the fabricated miniaturized OBT antenna; (d) Circuit diagram of the OBT circuit; (e) Diagram of the equivalent circuit model of the OBT circuit; (f)–(h) Simulated and measured reflection coefficient, gain, and power added efficiency (PAE) of the miniaturized OBT antenna.

linearly modulated by the term C_C, which represents the parasitic capacitor between the gate and the drain. As derived in [38], the gate-drain capacitor is negligible compared to other parasitic capacitors. Therefore, the impedance of the OBT antenna is majorly determined by the drain resistor R_D and parasitic capacitor C_D, which agrees well with previously introduced concept. On the other hand, Z_A, determined by the antenna element's geometry, has a minor effect on the impedance matching of the OBT antenna. Furthermore, the receiving gain of the antenna is also derived through this model. The gain of the OBT antenna is expressed as

$$G_{\mathrm{OBT}} = \frac{V_A g_m}{1+\omega C_G 50\cot\left(\frac{\pi l}{\lambda}\right)+\mathrm{j}\omega C_G 80\left(\frac{\pi l}{\lambda}\right)^2}\left(R_D+\frac{1}{\mathrm{j}\omega C_D}\right) \tag{3}$$

where V_A represents the voltage that the antenna element couples from the free space, l represents the length of the OBT antenna element, and λ stands for the free-space wavelength. According to (2), the overall gain of the OBT antenna increases proportionally with the antenna size. With the above derivations, the performance characteristics of the OBT antenna are analyzed. The operating frequency of the OBT antenna is minimally affected by its size, while enlarging its size increases the receiving gain. This characteristic overturns the fundamental physics on the relation between antenna size and its operating frequency, introducing geometry as a new degree of freedom into antenna design. Moreover, this decoupling allows the OBT antenna to be extremely miniaturized while maintaining its operating frequency.

2. Antenna miniaturization with OBT

As previously derived, the geometry of the antenna element has a minor effect on the operating frequency of the OBT antenna. Therefore, it is reasonably assumed that the size of the OBT antenna can be extremely miniaturized while still being effective at receiving signals. As a proof of concept, a schematic of the designed miniaturized OBT antenna is illustrated in Figure 2(a). As shown, the antenna element is extremely miniaturized to a microstrip line with a size of 1.36 mm × 0.75 mm ($0.00045\lambda_0 \times 0.00025\lambda_0$, where λ_0 is the free-space EM wavelength at 100 MHz), so the circuit effectively has no visible antenna part in the diagram. The antenna is printed on an FR-4 epoxy board ($\varepsilon_r = 4.4$, $\tan\delta = 0.02$) with a thickness of 0.6 mm and an overall size of 5 mm × 5 mm ($0.00167\lambda_0 \times 0.00167\lambda_0$). The OBT circuit is printed on the top side of the board with electronic elements soldered. The circuit diagram of the miniaturized OBT antenna is illustrated in Figure 2(d). It is important to note that the OBT circuit differs from the conventional transistor-based amplifiers in three significant ways. First, whereas amplifiers aim for high gain by biasing transistors in the saturation region to enhance signal boosting, the OBT circuit operates in the ohmic region to maintain stable impedance across the frequency spectrum. Second, conventional amplifiers typically require additional input and output matching circuits to reduce return loss, whereas the OBT circuit inherently performs active impedance matching without the need for supplementary elements. Third, traditional amplifiers often incorporate feedback loops to ensure stability and prevent self-excitation, whereas the ohmic region bias of the OBT circuit ensures intrinsic stability.

The geometry of the miniaturized OBT antenna is illustrated in Figure 2(b). The antenna element is labeled in red with length $l_e = 1.36$ mm and width $w_e = 0.75$ mm. The detailed geometries of the rest of the circuit are as the followings: $w_l = 0.5$ mm, $w_2 = 0.76$ mm, $l_1 = 0.74$ mm, $l_2 = 0.9$ mm, $l_3 = 1.32$ mm, $l_4 = 0.82$ mm, $l_5 = 0.9$ mm, and $l_6 = 0.47$ mm. Figure 2(c) shows a photograph of the fabricated miniaturized antenna. As illustrated, the miniaturized OBT antenna has an extremely small size compared to the general antennas seen in wireless systems. We simulate the reflection coefficient and gain of the miniaturized OBT antenna with commercial software High Frequency Structure Simulator (HFSS) and Microwave Office. Specifically, during operation, the capacitive antenna element forms a voltage division with the gate capacitor of the OBT, coupling the sensed electric field to the gate. The field effect of the OBT then converts the gate voltage to the drain current to the output port. Hence, the gain of the antenna is calculated as

$$G_{\mathrm{OBT}} = G_{\mathrm{ANT}} \times \frac{C_G}{C_G + C_A} \times G_{\mathrm{FET}} \div L_{\mathrm{mismatch}} \tag{4}$$

where G_{ANT} is the intrinsic gain of the antenna element, G_{FET} is the gain provided by the OBT during field effect, and $L_{\mathrm{mismatch}} = \sqrt{1-S_{11}^2}$ is the power loss of the antenna element due to impedance mismatch. The power added efficiency (PAE) yields

$$\eta = \frac{P_{\mathrm{in}} - P_{\mathrm{out}}}{P_{\mathrm{dc}}} \tag{5}$$

where P_{in} and $\mathrm{P}_{\mathrm{out}}$ are the input and output power of the OBT antenna, respectively; P_{dc} is the DC power consumption of the OBT antenna.

The simulated and measured reflection coefficients are illustrated in Figure 2(f). The miniaturized OBT antenna possesses a matched impedance from 100 MHz to 1.81 GHz with a reflection coefficient lower than –10 dB. This reveals that the miniaturized OBT antenna has an ultra-wide bandwidth. Using the calculation method shown in (4) and (5), we simulate and measure the gain and efficiency of the miniaturized OBT antenna. Figure 2(g) shows the gain curves of the miniaturized OBT antenna. As illustrated, the gain of the miniaturized OBT antenna ranges from –45.1 dBi to –21 dBi, demonstrating a notable gain improvement for such a small size. As shown in Figure 2(h), the antenna reaches a peak total efficiency of 2.16%. It should be noticed that this efficiency is higher than small antennas with similar sizes with different methodologies [20], [21], repre-

senting an acceptable radiation. This miniaturized antenna possesses an extremely small size at milli-wavelength scale as a chip and an ultra-wide bandwidth while maintaining compatibility with widely utilized PCB-based wireless systems. It is noticeable that the current configuration focuses on receive-only functionality. The proposed miniaturized OBT antenna in its current form could be utilized in communications scenarios such as broadcast receiving, positioning, or navigation. Moreover, incorporating technologies such as reconfigurable antennas could potentially extend the design's capability to support transmission as well.

Table 1 compares the performance of the miniaturized OBT antenna with four other state-of-the-art antennas featuring extremely miniaturized scale. For contrast, a well-designed regular antenna is also presented in Table 1. The comparison demonstrates that the antennas with miniaturization technology possess significant smaller scale than the regular antenna. Among the comparison, two ME antenna designs are proposed utilizing the AlN/FeGaB material, realizing miniaturized antenna with milli-wavelength scale. However, it is clearly observed that the ME antenna bandwidth is narrow, and their DC bias coils would cause extra volume occupation. As illustrated in Table 1, active antennas using non-Foster circuits reach a wide bandwidth within a small volume. However, antennas realized with non-Foster circuits possess a relatively large scale around 10^{-2} wavelength, making them unsuitable for systems with extreme volume requirement. On the other hand, as shown in Table 1, the miniaturized OBT antenna developed in this work possesses a much smaller scale, with milli-wavelength overall size, and an antenna element size of 10^{-4} wavelength scale. Not only does OBT antenna in this work possess a much wider bandwidth, but it also reaches a volume miniaturization of two orders of magnitude. Notably, the OBT antenna is different from non-Foster antennas in a number of aspects. First, the fundamental matching principles are different. Non-Foster antennas use non-Foster circuits with negative inductance or capacitance to match the impedance of small antennas, while OBT antennas achieve impedance matching by utilizing the resistance feature of the field effect transistor (FET) channel in the ohmic region. Second, the circuit structures are not the same. Non-Foster circuits typically use two identical FETs or bipolar junction transistors (BJTs) biased in the saturation region, whereas the OBT antenna design uses only a single FET biased in the ohmic region. Third, the matching bandwidths are not comparable. Non-Foster circuits typically operate within a narrow bandwidth, while the OBT antenna's FET channel resistance remains stable across a broader frequency range, enabling wideband impedance matching. Compared to regular antennas, this antenna has a reduced size by three orders of magnitude, and additionally demonstrating one to two orders of magnitude miniaturization over the state-of-the-art ME antennas and non-Foster circuit technologies, while realizing an ultra-wide bandwidth. It is noticeable that the antenna efficiency is relatively low at lower frequencies. However, in the calculation of the PAE, both the radiation gain of the antenna and the performance of the OBT circuit are considered. Consequently, the low PAE at lower frequencies is primarily due to the compact size and high loss of the antenna. Measurement results reveal that the OBT circuit itself possesses a PAE of 56%. Notably, the proposed antenna is approximately one order of magnitude smaller than state-of-the-art compact antennas reported in the literature. Given this significant size miniaturization, the efficiency remains acceptable. Moreover, the PAE of the OBT antenna can be further improved by increasing the antenna size.

Table 1 Performance comparison of the miniaturized OBT antenna and other published small antennas

Reference	Antenna type	Area ($\lambda_0 \times \lambda_0$)	Bandwidth	PAE	Processing
Zhang *et al.* [10]	Regular antenna	0.47 × 0.47	22.2%	N/A	PCB
Nan *et al.* [20]	ME antenna	0.0067 × 0.0058 (without bias coil)	0.4%	0.28% (2.5 GHz)	AlN/FeGaB
Zaeimbashi *et al.* [21]	ME antenna	0.002 × 0.0062 (without bias coil)	0.3%	5.4% (2.5 GHz)	AlN/FeGaB
Chen *et al.* [27]	Non-Foster antenna	Length: 0.048	40.7%	6.5% (650 MHz)	PCB
Zhu *et al.* [28]	Non-Foster antenna	0.1 × 0.08	49.2%	N/A	PCB
Sussman-Fort *et al.* [29]	Non-Foster antenna	Length: 0.02	143%	21.1% (21.4 MHz)	PCB
This work	**OBT antenna**	**0.00167 × 0.00167 (overall)** **0.00045 × 0.00025 (antenna element)**	**179%**	0.11%–2.2%*	**PCB**

Note: *The PAE of the miniaturized OBT antenna are 0.11% at 100 MHz, 0.76% at 500 MHz, and 2.2% at 1 GHz.

III. Discussion

1. Parametric discussion on OBT antennas

A parametric discussion is conducted to further validate the characteristics of the OBT antenna. Figure 3(a) illustrates the photograph of the fabricated OBT antennas, which are constructed by integrating antenna elements of different sizes with OBT circuits. ANT 1, ANT 2, and ANT 3 represent the OBT antenna with dimensions of 20 mm × 20 mm, 40 mm × 40 mm, and 80 mm × 80 mm, respectively. The OBT circuit is identical to the circuit diagram illustrated in Figure 2(c). The simulated and measured reflection coefficients of the different antennas are shown in Figure 3(b). As shown, ANT 1, ANT 2, and ANT 3 cover the operating fre-

quency range from 100 MHz to 1.85 GHz, 1.91 GHz, and 2.00 GHz, respectively. The bandwidth results indicate that geometrical size introduces a neglectable effect of approximately 2% on the operating bandwidth of OBT antennas. Conventional antennas operate through resonance, of which the resonating wavelength is determined by the boundary conditions defined by the antenna geometry. As a result, the operating frequency of conventional antennas is primarily defined by their geometric size. In contrast, the output impedance of the OBT antenna is governed by the FET drain impedance, and the antenna size has minimal effect on this impedance due to the one-way transmission feature of the FET. Consequently, the bandwidth of the OBT antenna is only marginally affected by its size. The gain simulation and measurement results are depicted in Figure 3(c). ANT 1 possesses a gain of −25.65 dBi to −1.75 dBi, while ANT 2 and ANT 3 have gains of −12 dBi to 4.45 dBi and −4.15 dBi to 9.42 dBi, respectively. It is clearly observed that the receiving gain increases with the antenna size. The results align well with the derivation in (3). The PAE of the antennas are illustrated in Figure 3(d). Receiving PAE of 11.5%, 24.0%, and 41.8% are achieved.

In summary, altering the size of the OBT antenna has a minor effect on its operating frequency. On the other hand, enlarging the size of the OBT antenna increases its receiving gain. The results provide a guideline for wideband and miniaturized antenna design. Unlike the conventional antenna design, which incorporates joint optimization of the antenna geometry, operating frequency, and gain, the OBT integration method decouples the antenna size from its operating frequency. Designers using the OBT integration method would select antenna geometry solely dependent on its gain requirement, without concerning for its operating frequency.

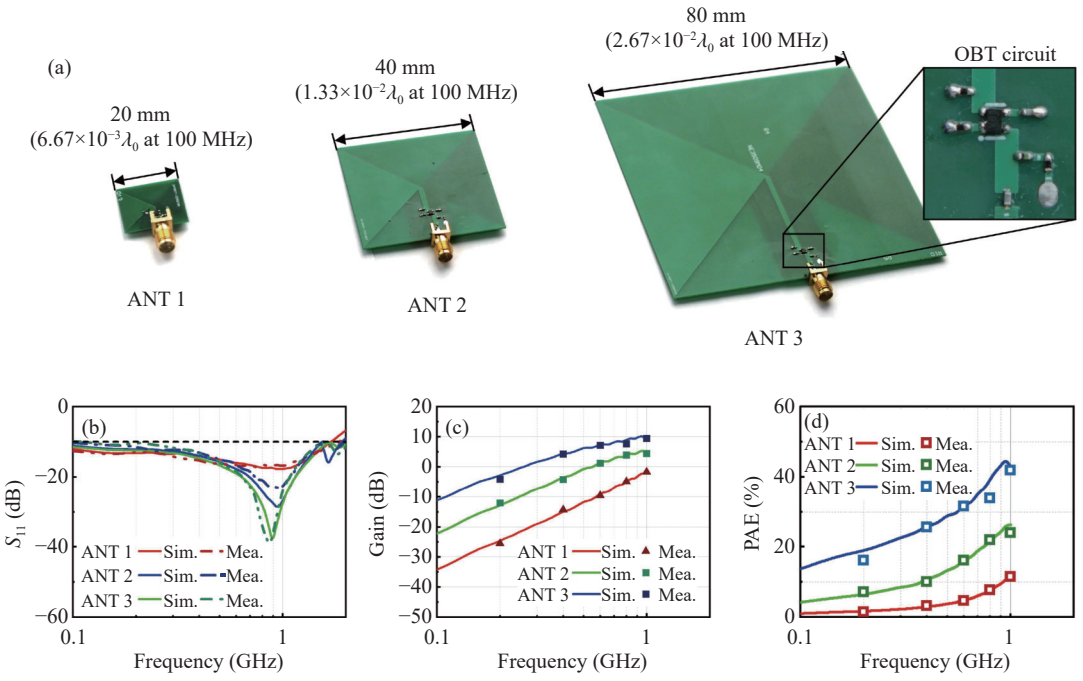

Figure 3 Numerical analysis and experimental verifications of the OBT antenna. (a) Photographs of the fabricated OBT antennas with different sizes; (b)–(d) Simulated and measured (b) Reflection coefficient, (c) Gain, and (d) PAE results of the OBT antennas.

2. Miniaturized OBT antenna demonstrations

As demonstrated in the preceding sections through theoretical derivations and verifications, the miniaturized OBT antenna possesses acceptable receiving performance despite its extremely miniaturized dimensions. To validate its performance and potential, two demonstration systems are built using the miniaturized OBT antenna: a sound transmission system and a video transmission system. A sketch of the sound transmission demonstration system is depicted in Figure 4(a). The speaker generates voice into an interphone with a monopole antenna serving as the transmission antenna, while the listener holds an interphone from a distance. The configurations of the receiving interphone with different antennas are illustrated in Figure 4(b). For comparison, ANT 1 represents a solder pad with a diameter of 2 mm, which acts as the receiving antenna with similar size to the antenna element of the miniaturized OBT antenna. ANT 2 is the miniaturized OBT antenna proposed in this work, with an overall size of 5 mm × 5 mm and antenna element size of 1.36 mm × 0.75 mm, and ANT 3 is a regular monopole antenna with a length of 115 mm. The demonstration utilizes Xiaomi XMDJJL01 interphones. Both interphones communicate at the 400 MHz frequency band. The distances are measured for the different receiving antennas based on the reception of no signal, noise signal, or clear signal. As illustrated in Figure 4(c), ANT 1 receives a clear signal from 0 m to 89 m, which degrades into a noise signal

from 89 m to 146 m, and no signal beyond 146 m. ANT 2 receives a clear signal within 489 m and a noise signal within 594 m. In contrast, a clear signal is received within 552 m utilizing ANT 3, and a noise signal within 701 m. It is worth mentioning that in both industrial and academic practice, the PCB board often serves as the radiator, though it is typically referred to as the "ground". In contrast, the so-called "antenna", such as the monopole antenna shown in Figure 4, functions as an impedance matching component. However, it is important to note that while the PCB board in the comparison is identical across all cases, the antenna itself exhibits a noticeable size difference.

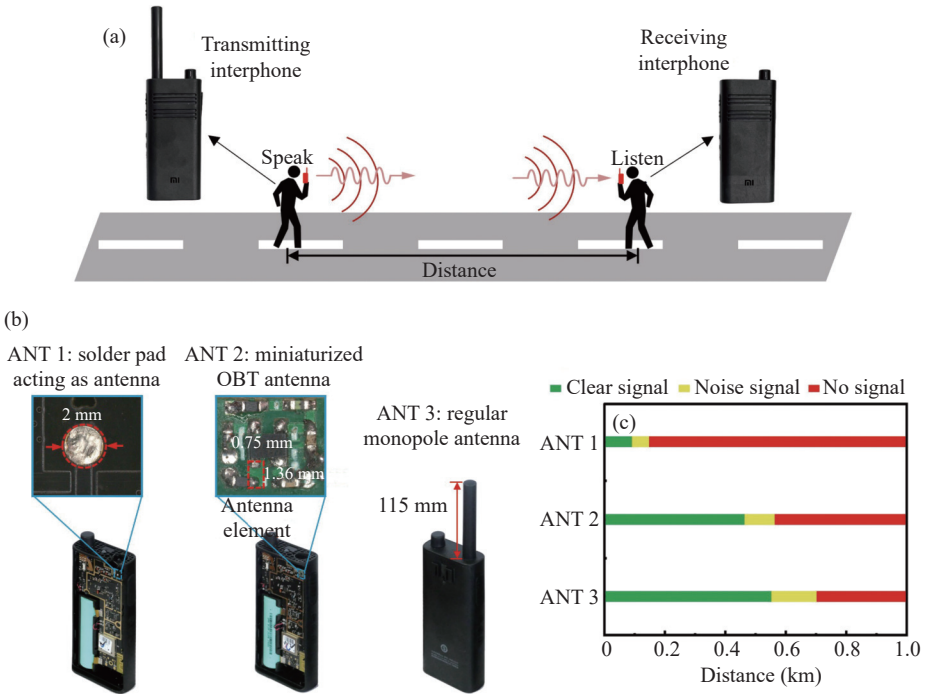

Figure 4 Interphone demonstration system. (a) Sketch of the sound transmission system using different receiving antennas. The speaker and the listener each holds an interphone with a distance; (b) Configuration of the utilized receiving interphones. ANT 1, ANT 2, and ANT 3 represent a solder pad acting as receiving antenna, the miniaturized OBT antenna with extremely small antenna element, and a regular monopole antenna, respectively; (c) Distance where ANT 1, ANT 2, and ANT 3 receive clear signal, noise signal, and no signal.

This validation demonstrates that, despite its extremely small dimensions, the miniaturized OBT antenna provides acceptable receiving performance. On the other hand, a significant improvement is introduced comparing to the conventional antenna (solder pad) of similar size. The configuration of the miniaturized OBT antenna also indicates a high compatibility with the widely applied PCB process.

Furthermore, to thoroughly demonstrate the advantage of the miniaturized OBT antenna over traditional passive antennas, a simulation is carried out for the scenario of interphone applications. The simulation setup is illustrated in Figure 5(a). To accurately model the EM structure of the interphone, the solder pad is placed on an FR-4 epoxy board with a thickness of 1 mm. Both sides of the board are covered with metal serving as the ground, with vias connecting them. The solder pad, acting as a monopole antenna with a diameter of 2 mm, is positioned at the corner of the circuit board. For comparison, the photograph of the interphone circuit board top view is shown in Figure 5(b), and the corresponding circuit diagrams for the simulated scenarios are provided in Figure 5(c). To compare radiation performance, we employ a pair of lossless serial and shunt inductors to match the solder pad at 400 MHz. The S_{11} parameters for the solder pad with OBT matching, passive matching, and without matching are depicted in Figure 5(d). As shown, the S_{11} of the solder pad without matching is close to 0 dB, indicating poor impedance matching. The passive matching technique achieves an S_{11} below –10 dB but within a narrow bandwidth. In contrast, OBT matching provides a significantly wider bandwidth. The simulated gains are presented in Figure 5(e). The results indicate that the solder pad without matching exhibits a significantly lower gain compared to the configurations with passive and active matching. Within the bandwidth of the passive-matched solder pad, its gain is comparable to that of the actively matched antenna. However, beyond this bandwidth, the gain of the passive-matched antenna is much lower than that of the OBT-matched configuration. Simulation results indicate that with OBT matching, the antenna achieves a gain comparable to traditional passive matching while exhibiting a significantly wider matched bandwidth. This validates the advantage of OBT matching in enabling ultra-wideband operation. Additionally, although the gain of the miniaturized OBT antenna is low, the results confirm that

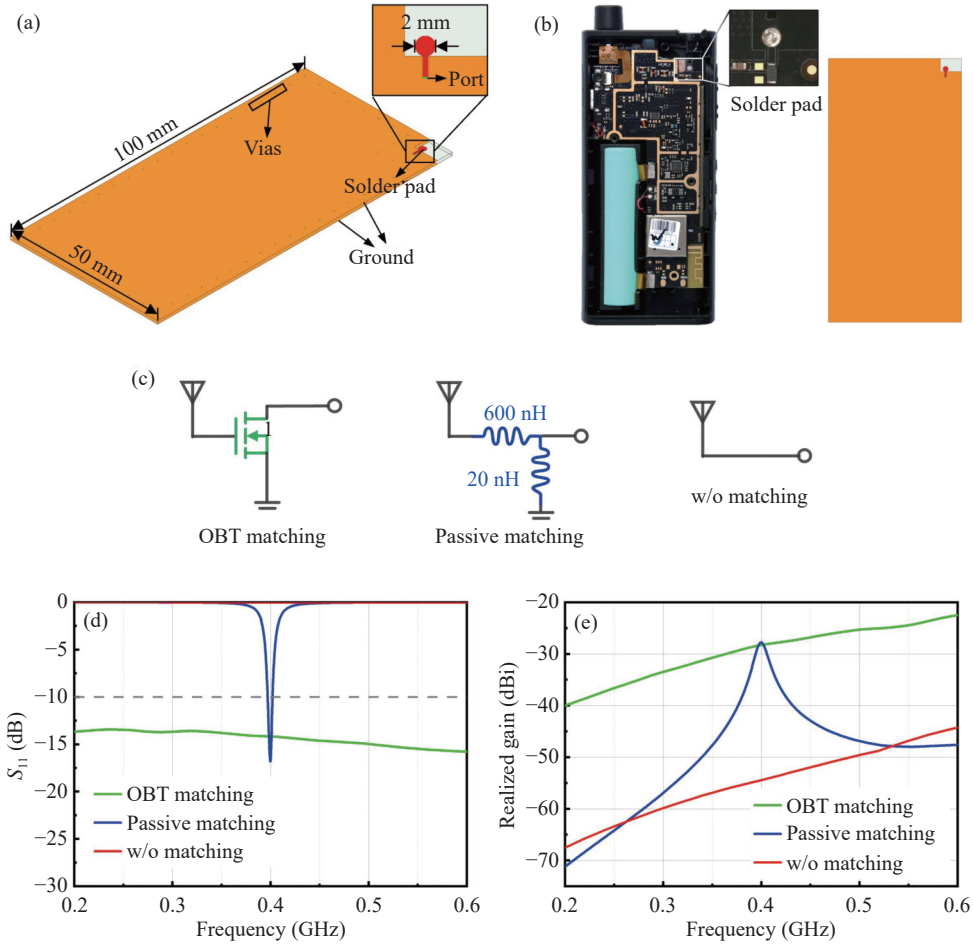

Figure 5 Simulation of the solder pad antenna in Figure 4. (a) Simulation setup of the solder pad antenna; (b) Top views of the interphone circuit board photograph and the simulation model; (c) Circuit diagrams of the solder pad antenna with OBT matching, with passive inductors matching, and without (w/o) matching; (d) Simulated S_{11} of the antenna with OBT matching, with passive matching, and without (w/o) matching; (e) Simulated realized gain of the antenna with OBT matching, with passive matching, and without (w/o) matching.

the primary cause of this low gain is the lossy FR-4 epoxy substrate rather than the OBT circuit. Further improvements in antenna gain could be achieved by designing an all-metal antenna or utilizing a substrate with lower loss.

A sketch of the video transmission system is shown in Figure 6(a). A pair of Universal Software Radio Peripherals (USRPs) controlled by laptops are utilized as the transmitter and receiver. The transmitter USRP utilizes a monopole antenna as the transmitting (TX) antenna, while the receiver USPR employs the miniaturized OBT antenna. The transmitted video is modulated with 16-quadrature amplitude modulation (16-QAM). As an example, the miniaturized OBT antenna is used to receive the video signals coming from different angles at 1 GHz. The received constellation diagrams are shown in Figure 6(b). The results indicate that the constellation diagrams received from different angles exhibit similar performance, demonstrating the isotropy of the miniaturized OBT antenna. The received constellation diagrams using the miniaturized OBT antenna at different frequencies are illustrated in Figures 6(c)–6(e). These diagrams indicate effective receiving across the operating band. These demonstrations validate the performance of the extremely miniaturized OBT antenna. The results indicate that the miniaturized OBT antenna is highly compatible with the hardware of wireless systems while possessing satisfactory receiving abilities. The demonstration reveals that the miniaturized OBT antenna can be utilized in multiple volume-limited scenarios, including but not limited to nanophotonic antennas [39], implant antennas [40], and drone-carried terminals [41].

IV. Conclusion

Antennas usually consume sufficient area for radiation due to the intrinsic relation between dimension and operating frequency. In this work, we develop the methodology of OBT integration to realize the well-radiated antennas with extremely small dimensions. We utilize the equivalent model to derive the impedance and gain of the OBT antennas, indicating that the antennas can be extremely miniaturized at the cost of gain, without altering their frequency. A miniaturized OBT antenna with milli-wavelength scales is designed with exciting numerical and experiment results, validating the relationship between the size of the OBT antenna with its gain and operating frequency. The miniatur-

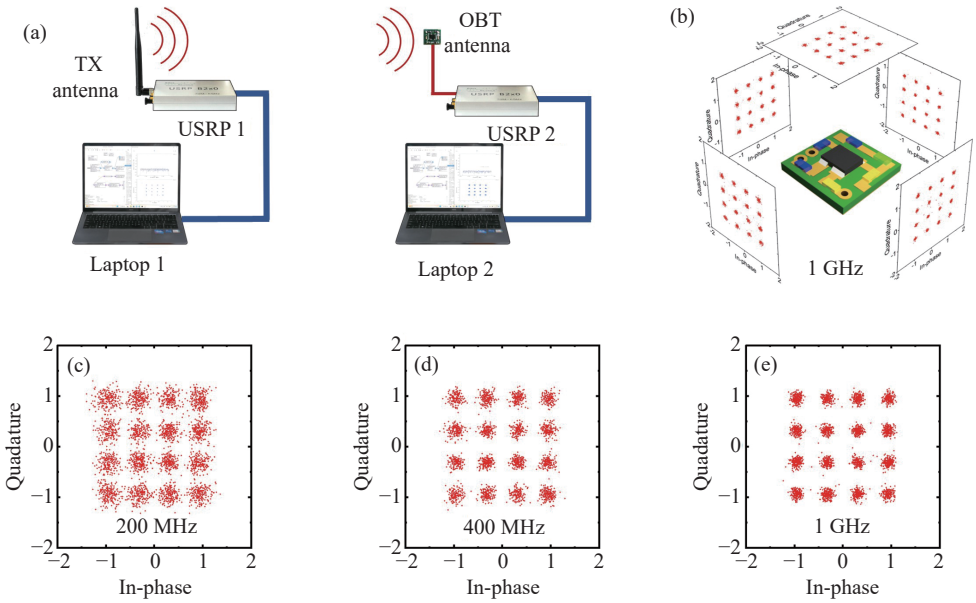

Figure 6 Video transmission demonstration system. (a) Block diagram of the video transmission system; (b) Constellation diagrams of the video transmission system using the OBT antenna at different angles at 1 GHz; Constellation diagrams of the video transmission system using the miniaturized OBT antenna at (c) 200 MHz, (d) 400 MHz, and (e) 1 GHz.

ized OBT antenna possesses an antenna element size of $1.36\ \text{mm}\times 0.75\ \text{mm}$ $(0.00045\lambda_0\times 0.00025\lambda_0)$, and takes an overall size of $5\ \text{mm}\times 5\ \text{mm}$ including the OBT circuit. Demonstration systems are built to prove that the OBT antenna possesses a high compatibility and satisfactory performance in the practical systems. This miniaturized OBT antenna would be broadly applied in various disciplines relying on deep-subwavelength wireless systems, the examples include fields of information technologies [32], photoelectricity physics [33], and biomedical science [34], among others [35], [36].

Acknowledgements

This work was supported by the National Key Research and Development Program of China (Grant No. 2021YFA 0716601) and the National Natural Science Foundation of China (Grant No. U22B2016).

References

[1] H. Li, Z. H. Zhou, Y. J. He, *et al*., "Geometry-independent antenna based on Epsilon-near-zero medium," *Nature Communications*, vol. 13, no. 1, article no. 3568, 2022.

[2] Y. Wang, L. B. Sun, Z. W. Du, *et al*., "Review antenna design for modern mobile phones: A review," *Electromagnetic Science*, vol. 2, no. 2, pp. 1–36, 2024.

[3] Y. P. Zhang, "Differential antennas: Fundamentals and applications," *Electromagnetic Science*, vol. 1, no. 1, article no. 0010021, 2023.

[4] Y. J. Zhang and Y. Li, "Wideband microstrip antenna in small volume without using fundamental mode," *Electromagnetic Science*, vol. 1, no. 2, article no. 0020073, 2023.

[5] H. Li, Z. H. Zhou, Y. Z. Zhao, *et al*., "Low-loss beam synthesizing network based on Epsilon-near-zero (ENZ) medium for on-chip antenna array," *Chip*, vol. 2, no. 2, article no. 100049, 2023.

[6] Z. H. Zhou, and Y. Li, "Frequency-division-multiplexing information transmission based on index-near-zero metamaterials," *Chinese Journal of Radio Science*, vol. 36, no. 6, pp. 905–911, 2021.

[7] M. Svanda and M. Polivka, "Matching technique for an on-body low-profile coupled-patches UHF RFID tag and for sensor antennas," *IEEE Transactions on Antennas and Propagation*, vol. 63, no. 5, pp. 2295–2301, 2015.

[8] G. P. Gao, B. K. Zhang, J. H. Dong, *et al*., "A compact dual-mode pattern-reconfigurable wearable antenna for the 2.4-GHz WBAN application," *IEEE Transactions on Antennas and Propagation*, vol. 71, no. 2, pp. 1901–1906, 2023.

[9] Y. J. He, Z. Z. Pan, X. D. Cheng, *et al*., "A novel dual-band, dual-polarized, miniaturized and low-profile base station antenna," *IEEE Transactions on Antennas and Propagation*, vol. 63, no. 12, pp. 5399–5408, 2015.

[10] Y. J. Zhang, Y. Li, W. Q. Zhang, *et al*., "Omnidirectional antenna diversity system for high-speed onboard communication," *Engineering*, vol. 11, pp. 72–79, 2022.

[11] M. Ignatenko and D. S. Filipovic, "On the design of vehicular electrically small antennas for NVIS communications," *IEEE Transactions on Antennas and Propagation*, vol. 64, no. 6, pp. 2136–2145, 2016.

[12] Z. Y. Liu, Y. J. Zhang, Y. J. He, *et al*., "A compact-size and high-efficiency cage antenna for 2.4-GHz WLAN access points," *IEEE Transactions on Antennas and Propagation*, vol. 70, no. 12, pp. 12317–12321, 2022.

[13] P. B. Samal, S. J. Chen, and C. Fumeaux, "3-D-corrugated ground structure: A microstrip antenna miniaturization technique," *IEEE Transactions on Antennas and Propagation*, vol. 72, no. 5, pp. 4010–4022, 2024.

[14] Z. Y. Liu, Y. J. He, and Y. Li, "Beamwidth enhancement of microstrip antennas using capacitive via-fence loading," *IEEE Open Journal of Antennas and Propagation*, vol. 4, pp. 151–158, 2023.

[15] P. Y. Fu, Y. J. Zhang, M. Z. Hu, *et al*., "A low-power-consumption massive MIMO scheme based on multibeam antenna array," *Microwave and Optical Technology Letters*, vol. 64, no. 8, pp. 1428–1433, 2022.

[16] Z. Li, Q. Z. You, H. Wang, *et al*., "Nanowire dimer optical antenna brightens the surface defects of silicon," *Nanophotonics*, vol. 12, no. 9, pp. 1723–1731, 2023.

[17] S. X. Gao, Y. B. Li, C. R. Ma, *et al*., "Emitting long-distance spiral airborne sound using low-profile planar acoustic antenna," *Nature Communications*, vol. 12, no. 1, article no. 2006, 2021.

[18] R. M. Bichara, J. Costantine, Y. Tawk, *et al*., "A multi-stable deployable quadrifilar helix antenna with radiation reconfigurability for disaster-prone areas," *Nature Communications*, vol. 14, no. 1, article no. 8511, 2023.

[19] Y. J. Zhang and Y. Li, "Scalable omnidirectional dual-polarized antenna using cavity and slot-dipole hybrid structure," *IEEE Transactions on Antennas and Propagation*, vol. 70, no. 6, pp. 4215–4223, 2022.

[20] T. X. Nan, H. Lin, Y. Gao, *et al*., "Acoustically actuated ultra-compact NEMS magnetoelectric antennas," *Nature Communications*, vol. 8, no. 1, article no. 296, 2017.

[21] M. Zaeimbashi, M. Nasrollahpour, A. Khalifa, *et al*., "Ultra-compact dual-band smart NEMS magnetoelectric antennas for simultaneous wireless energy harvesting and magnetic field sensing," *Nature Communications*, vol. 12, no. 1, article no. 3141, 2021.

[22] B. Joy, Y. B. Cai, D. C. Bono, *et al*., "Cell Rover—a miniaturized magnetostrictive antenna for wireless operation inside living cells," *Nature Communications*, vol. 13, no. 1, article no. 5210, 2022.

[23] X. Yang, Z. H. Zhang, M. W. Xu, *et al*., "Digital non-Foster-inspired electronics for broadband impedance matching," *Nature Communications*, vol. 15, no. 1, article no. 4346, 2024.

[24] S. E. Sussman-Fort, "Matching network design using non-Foster impedances," *International Journal of RF and Microwave Computer-Aided Engineering*, vol. 16, no. 2, pp. 135–142, 2006.

[25] P. Y. Chen, C. Argyropoulos, and A. Alù, "Broadening the cloaking bandwidth with non-Foster metasurfaces," *Physical Review Letters*, vol. 111, no. 23, article no. 233001, 2013.

[26] E. Ugarte-Munoz, S. Hrabar, D. Segovia-Vargas, *et al*., "Stability of non-Foster reactive elements for use in active metamaterials and antennas," *IEEE Transactions on Antennas and Propagation*, vol. 60, no. 7, pp. 3490–3494, 2012.

[27] H. C. Chen, H. Y. Yang, C. C. Kao, *et al*., "Slot antenna with non-Foster and negative conductance matching in consecutive bands," *IEEE Antennas and Wireless Propagation Letters*, vol. 18, no. 6, pp. 1203–1207, 2019.

[28] N. Zhu and R. W. Ziolkowski, "Active metamaterial-inspired broadbandwidth, efficient, electrically small antennas," *IEEE Antennas and Wireless Propagation Letters*, vol. 10, pp. 1582–1585, 2011.

[29] S. E. Sussman-Fort and R. M. Rudish, "Non-Foster impedance matching of electrically-small antennas," *IEEE Transactions on Antennas and Propagation*, vol. 57, no. 8, pp. 2230–2241, 2009.

[30] S. Y. Wang and Y. Li, "Single-transistor impedance matching circuit for over-hundred-octave active antennas," *IEEE Transactions on Antennas and Propagation*, vol. 72, no. 3, pp. 2391–2398, 2024.

[31] S. Y. Wang, Z. Y. Liu, Y. J. Zhang, *et al*., "Active-passive reconfigurable antenna covering 70–7200 MHz bandwidth," *IEEE Transactions on Antennas and Propagation*, vol. 72, no. 9, pp. 7323–7328, 2024.

[32] T. S. Rappaport, Y. C. Xing, G. R. MacCartney, *et al*., "Overview of millimeter wave communications for fifth-generation (5G) wireless networks—with a focus on propagation models," *IEEE Transactions on Antennas and Propagation*, vol. 65, no. 12, pp. 6213–6230, 2017.

[33] P. Sanjari and F. Aflatouni, "An integrated photonic-assisted phased array transmitter for direct fiber to mm-wave links," *Nature Communications*, vol. 14, no. 1, article no. 1414, 2023.

[34] Z. X. Li, X. H. Guo, Y. Jin, *et al*., "Atomic optical antennas in solids," *Nature Photonics*, vol. 18, no. 10, pp. 1113–1120, 2024.

[35] S. Castilla, I. Vangelidis, V. V. Pusapati, *et al*., "Plasmonic antenna coupling to hyperbolic phonon-polaritons for sensitive and fast mid-infrared photodetection with graphene," *Nature Communications*, vol. 11, no. 1, article no. 4872, 2020.

[36] Z. H. Yao, X. Z. Chen, L. Wehmeier, *et al*., "Probing subwavelength in-plane anisotropy with antenna-assisted infrared nano-spectroscopy," *Nature Communications*, vol. 12, no. 1, article no. 2649, 2021.

[37] C. A. Balanis, *Antenna Theory—Analysis and Design*, 4th ed., John Wiley & Sons, Hoboken, NI, USA, 2016.

[38] D. A. Neamen, *Semiconductor Physics and Devices: Basic Principles*, 4th ed., McGraw-Hill, New York, NY, USA, 2012.

[39] J. Sun, E. Timurdogan, A. Yaacobi, *et al*., "Large-scale nanophotonic phased array," *Nature*, vol. 493, no. 7431, pp. 195–199, 2013.

[40] K. Kwon, J. U. Kim, S. M. Won, *et al*., "A battery-less wireless implant for the continuous monitoring of vascular pressure, flow rate and temperature," *Nature Biomedical Engineering*, vol. 7, no. 10, pp. 1215–1228, 2023.

[41] Z. Y. Yu, X. L. Hu, C. X. Liu, *et al*., "Location sensing and beamforming design for IRS-enabled multi-user ISAC system," *IEEE Transactions on Signal Processing*, vol. 70, pp. 5178–5193, 2022.

Shuyu Wang received the B.S. degree in electronic engineering from Tsinghua University, Beijing, China, in 2022, where he is currently pursuing the Ph.D. degree in electronic engineering. His current research interests include electrically small antennas, active circuits, and wideband active antennas.

Mr. Wang serves as a reviewer for *IEEE Transactions on Antennas and Propagation* and *Microwave and Optical Technology Letters*.
(Email: wsy22@mails.tsinghua.edu.cn)

Yongjian Zhang received the B.S. degree in communication engineering from Tongji University, Shanghai, China, in 2018, and the Ph.D. degree in electronic engineering from Tsinghua University, Beijing, China, in 2023. He is currently a Post-Doctoral Fellow with the Department of Electronic Engineering, Tsinghua University, Beijing, China. His current research interests include aircraft antennas, dual-polarized antennas, and multiple-input and multiple-output (MIMO) antenna arrays.

Dr. Zhang serves as a reviewer for *IEEE Transactions on Antennas and Propagation*, *IEEE Antennas and Wireless Propagation Letters*, and *Microwave and Optical Technology Letters*.
(Email: zhangyj18@mails.tsinghua.edu.cn)

Zhenyu Liu received the B.S. degree in electronic engineering from Tsinghua University, Beijing, China, in 2022, where he is currently pursuing the Ph.D. degree in electronic engineering. His current research interests include electrically small antennas, active circuits, and wideband active antennas.
(Email: liuzy20@mails.tsinghua.edu.cn)

Jinlong Zhang received the B.S. degree in communication engineering from Shenyang Ligong University, Shenyang, China, in 2022. He is currently working with Beijing National Research Center for Information Science and Technology, Beijing, China.
(Email: zjlong@mail.tsinghua.edu.cn)

Ziheng Zhou received the B.S. degree in physics from Nanjing University, Nanjing, China, in 2017 and the Ph.D. degree in electronic engineering from Tsinghua University, Beijing, China, in 2022. He is currently working with the College of Physics and Information Engineering, Fuzhou University, Fuzhou, China. His research interests include metamaterials, artificial index-near-zero media, electromagnetic absorbers, MIMO antennas, and metamaterial-assisted antennas.

Dr. Zhou received the Best Paper Award from the International Symposium on Antennas and Propagation (ISAP) in 2019, the Young Researcher Award from the Chinese Metamaterial Conference in 2019, and the Outstanding Ph.D. Thesis Award from Tsinghua University, Beijing, China, in 2022. He is serving as a Reviewer for *IEEE Transactions on Antennas and Propagation* and *IEEE Antennas and Wireless Propagation Letters*.
(Email: zhouzh@fzu.edu.cn)

Wenhua Chen received the B.S. degree in microwave engineering from University of Electronic Science and Technology of China (UESTC), Chengdu, China, in 2001 and the Ph.D. degree in electronic engineering from Tsinghua University, Beijing, China, in 2006.

From 2010 to 2011, he was a Post-Doctoral Fellow with iRadio Laboratory, University of Calgary, Calgary, AB, Canada. He is currently a Full Professor with the Department of Electronic Engineering, Tsinghua University, Beijing, China. He has authored or coauthored over 200 journal articles and conference papers. His main research interests include energy-efficient power amplifiers (PA) and linearization, and millimeter-wave integrated circuits.

Dr. Chen was a recipient of the 2015 Outstanding Youth Science Foundation of the National Natural Science Foundation of China, the 2014 URSI Young Scientist Award, and the Student Paper Awards of several international conferences. He is currently an Associate Editor of *IEEE Microwave and Wireless Components Letters* and an Editorial Member of *Engineering*. He was an Associate Editor of *IEEE Transactions on Microwave Theory and Techniques*.
(Email: chenwh@tsinghua.edu.cn)

Zhijun Zhang received the B.S. and M.S. degrees from University of Electronic Science and Technology of China, Chengdu, China, in 1992 and 1995, respectively, and the Ph.D. degree from Tsinghua University, Beijing, China, in 1999. In 1999, he was a Post-Doctoral Fellow with the Department of Electrical Engineering, University of Utah, Salt Lake City, UT, USA, where he was appointed as a Research Assistant Professor in 2001. In 2002, he joined University of Hawaii at Manoa, Honolulu, HI, USA, as an Assistant Researcher, and Amphenol T&M Antennas, Vernon Hills, IL, USA, as a Senior Staff Antenna Development Engineer, and was then promoted as an Antenna Engineer Manager. In 2004, he joined Nokia Inc., San Diego, CA, USA, as a Senior Antenna Design Engineer. In 2006, he joined Apple Inc., Cupertino, CA, USA, as a Senior Antenna Design Engineer and was then promoted to a Principal Antenna Engineer. Since 2007, he has been with Tsinghua University, Beijing, China, where he is currently a Professor with the Department of Electronic Engineering. He has authored *Antenna Design for Mobile Devices* (Wiley, 1st ed. 2011, 2nd ed. 2017).

Dr. Zhang served as an Associate Editor of *IEEE Transactions on Antennas and Propagation* from 2010 to 2014 and *IEEE Antennas and Wireless Propagation Letters* from 2009 to 2015.
(Email: zjzh@tsinghua.edu.cn)

Xi Chen received the B.S. degree in telecommunication engineering from Beijing University of Posts and Telecommunications, Beijing, China, in 2001 and the Ph.D. degree from Tsinghua University, Beijing, China, in 2006. He is currently with Beijing National Research Center for Information Science and Technology, Beijing, China, as an Associate Professor. His research interests include synergy of satellite communication and navigation and massive signals of opportunity positioning.
(Email: chenxiee@tsinghua.edu.cn)

Kunpeng Wei received the B.S. degree in electronic and information engineering from Huazhong University of Science and Technology, Wuhan, China, in 2008 and the Ph.D. degree in electrical engineering from Tsinghua University, Beijing, China, in 2013.

In 2012, he was a Visiting Scholar with the School of Electrical and Computer Engineering, Georgia Institute of Technology, Atlanta, GA, USA. From Jul. 2013 to Dec. 2015, he was employed in Radar Research Institute of Chinese Air Force Research Laboratory, conducting research in the areas of phased-array antenna design and radar system design. He joined Consume Business Group of Huawei Inc. in 2016, where he had been an Antenna Specialist and the Director of Xi'an Antenna Team. Since 2021, He joined Honor Device Co., Ltd. when this company split from Huawei and he was the Director of Honor Antenna Team. After leaving Honor, he joined Xiaomi Corporation, Beijing, China, in 2023. He is currently the Chief Antenna Expert and the Head of the Antenna Technology Team. He leads a large group of antenna experts and engineers and takes the full responsibility in the research of antenna technologies to guarantee the market success of all Xiaomi's products ranging from smartphones, electric cars, tablets, and other Internet-of-things devices. He has authored over referred 60 papers on consumer electronics antenna design. He holds over 100 granted U.S./EU/JP/CN patents and has other 20+ patent applications in pending. His current research interests include MIMO antenna technology, satellite communication technology, 5.5 GHz/millimeter wave technology, ultra-wide-band (UWB) wireless technology and meta-antennas for "Human x Car x Home" smart ecosystem.

Dr. Wei is an IET Fellow. He was a recipient of the Principal Scholarship of Tsinghua University in 2012, the Huawei Individual Gold Medal Award in 2018, the Huawei Team Gold Medal Award in 2017, and the Honor Team Gold Medal Award in 2021, respectively. He has been served as an Associate Editor of *IET Electronic Letters* since Oct. 2021 and *IEEE Open Journal of Antennas and Propagation* since Oct. 2023. He is also a Special Level External Expert of China Academy of Information and Communications Technology, Beijing, China. He is also an Adjunct Professor with the School of Electronics and Information Engineering, Shenzhen University, Shen-

zhen, China.
(Email: weikunpeng_2013@tsinghua.org.cn)

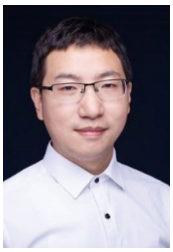

Yue Li received the B.S. degree in telecommunication engineering from Zhejiang University, Hangzhou, China, in 2007, and the Ph.D. degree in electronic engineering from Tsinghua University, Beijing, China, in 2012.

He is currently an Associate Professor with the Department of Electronic Engineering, Tsinghua University, Beijing, China. In June 2012, he was a Postdoctoral Fellow with the Department of Electronic Engineering, Tsinghua University, Beijing, China. In December 2013, he was a Research Scholar with the Department of Electrical and Systems Engineering, University of Pennsylvania, Philadelphia, PA, USA. He was also a Visiting Scholar with the Institute for Infocomm Research (I2R), A*STAR, Singapore, in 2010, and the Hawaii Center of Advanced Communication (HCAC), University of Hawaii at Manoa, Honolulu, HI, USA, in 2012. He has authored and coauthored over 235 journal papers and 50 international conference papers, and holds 26 granted Chinese patents. His current research interests include metamaterials, plasmonics, electromagnetics, nanocircuits, mobile and handset antennas, MIMO and diversity antennas, and millimeter wave antennas and arrays.

Dr. Li was a recipient of the Issac Koga Gold Medal from URSI General Assembly in 2017; the Young Scientist Award from the conferences of Progress in Electromagnetics Research Symposium (PIERS) 2019, International Applied Computational Electromagnetics Society Symposium (ACES) 2018, Atlantic Radio Science Conference (AT-RASC) 2018, Asia-Pacific Radio Science Conference (AP-RASC) 2016, International Symposium on Electromagnetic Theory (EMTS) 2016, and URSI General Assembly and Scientific Symposium (GASS) 2014. He served as an Associate Editor for *IEEE Transactions on Antennas and Propagation* and *IEEE Antennas and Propagation Letters* from 2017 to 2024. He is serving as an Associate Editor for *Microwave and Optical Technology Letters* and *Computer Applications in Engineering Education*.

(Email: lyee@tsinghua.edu.cn)